
CMAC-based modelling for HPDDL welding process control

Peiyong Duan

School of Information and Electrical Engineering,
Shandong Institute of Architecture and Engineering,
Jinan 250101, Shandong, China
E-mail: dpy2005@hotmail.com

Yu Ming Zhang*

Department of Electrical and Computer Engineering,
Center for Manufacturing,
University of Kentucky,
Lexington, KY 40506, USA
E-mail: ymzhang@engr.uky.edu

*Corresponding author

Abstract: A Cerebellar Model Articulation Controller- (CMAC-) based modelling method and closed-loop control system were developed to estimate and control the weld fusion for measuring the topside and backside bead widths of the weld pool in High Power Direct Diode Laser (HPDDL) welding. Because of the difficulty in using backside sensor, a topside weld pool geometry is measured using a topside vision sensor and is also used to measure the backside bead width. The drive current of the laser and the welding speed are taken as the control variables. The basic function of CMAC-based steady-state models, which are more easily obtained than dynamic ones, of the non-linear controlled process can predict the control variables with satisfactory accuracy to shorten output response transient time, and two simple Proportional and Integral (PI) controllers are included in the control system to adjust the control variables to maintain outputs at the desired levels. The results of closed-loop control simulations of laser welding process demonstrate that the developed control system is effective and robust to fluctuations or variations that lead to the changing parameters of the non-linear model.

Keywords: neurocontrol; laser welding; modelling; non-linear systems.

Reference to this paper should be made as follows: Duan, P. and Zhang, Y.M. (2006) 'CMAC-based modelling for HPDDL welding process control', *Int. J. Modelling, Identification and Control*, Vol. 1, No. 2, pp.107–114.

Biographical notes: Peiyong Duan received his PhD in Control Theory and Control Engineering from Shanghai Jiao Tong University, Shanghai, China in 1999. He received his MS and BS in Automatic Control from Shandong University in 1996 and Shandong Institute of Architecture and Engineering (SIAE), Jinan, China in 1991. As a Professor of Electrical Engineering at SIAE, currently, he is pursuing cooperative research at the University of Kentucky Welding Research Laboratory. His research interest includes non-linear system identification, modelling and control, especially intelligent control in industrial process and intelligent building system.

Yu Ming Zhang is a Professor and the Director of Graduate Studies in the Department of Electrical and Computer Engineering at the University of Kentucky where he holds the James R. Boyd Professorship in Electrical Engineering and directs the Welding Research Laboratory and Applied Sensing and Control Laboratory. He received his PhD in Mechanical Engineering/Welding Major and MS and BS in Electrical Engineering/Control Major from the Harbin Institute of Technology, Harbin, China. He is a senior member of the IEEE and the SME and a member of the AWS and the ASME. He received the Donald Julius Groen Prize from the Institution of Mechanical Engineers, UK, the AF Davis Silver Medal award and the Adams Memorial Membership Award from the American Welding Society and the 15th IFAC Triennial World Congress Poster Paper Prize and Application Paper Honorable Mention from the International Federation of Automatic Control.

1 Introduction

With the increasing applications of industrial lasers in welding, the demand for high productivity and quality assurance becomes urgent. One of the key issues is to find advanced control methods associated with different laser production processes. For Nd:YAG and CO₂ laser welding, some systems have been developed to control laser power, welding speed and focal point of lasers (Bagger and Olsen, 2003; Bardin et al., 2005; Kawahito and Katayama, 2004; Meijer et al., 2002). High Power Direct Diode Laser (HPDDL) is a new type of heat source, and has started replacing conventional lasers for certain seam welding applications. Owing to its high efficiency, HPDDL is very compact and can be mounted directly on to a tube mill or robot enabling high-speed and high-quality welding of both ferrous and non-ferrous metals. All these solid-state laser systems inherently provide the ability to control the output laser energy with a degree that is unmatched by conventional Nd:YAG and CO₂ lasers. The Welding Research Laboratory at the University of Kentucky has equipped this type of laser for welding experiments with custom designed measurement and control system for real-time monitoring and control of welding quality. As laser-welding process is a strong non-linear system subject to disturbances, the design of control system might be difficult. In addition, existing welding control systems focus on their own aspects pertinent to that particular welding process through choosing different operational variables according to the lasers used and the workpiece to be processed. In fact, HPDDL has a different laser profile, 12 mm × 0.5 mm, production mechanism being different from other kinds of lasers such as Nd:YAG and CO₂ lasers. This beam profile is not 'keyhole', thus yielding higher quality seam welding process. Therefore, present control systems for keyhole process could not be directly used in HPDDL welding processes.

This research concentrates on controlling the fusion state of fully penetrated welds in the HPDDL welding process with a 12 mm × 0.5 mm profile. The welding speed and the laser drive current are selected as control variables. The weld pool topside width and backside width, which measures the weld penetration, are two critical parameters reflecting the weld quality and need to be controlled simultaneously and are selected as the system outputs. The control system to be studied is thus more complicated than either pool width control or penetration control. In order to enable the welding process control system to use the instantaneous feedback information of the weld geometry, a high-shutter-speed camera assisted with a pulse laser is installed to capture weld pool images that are processed online to get the weld pool boundary. This image capturing method has been successfully applied to Gas Tungsten Arc (GTA) welding control system in our lab (Zhang and Kovacevic, 1998).

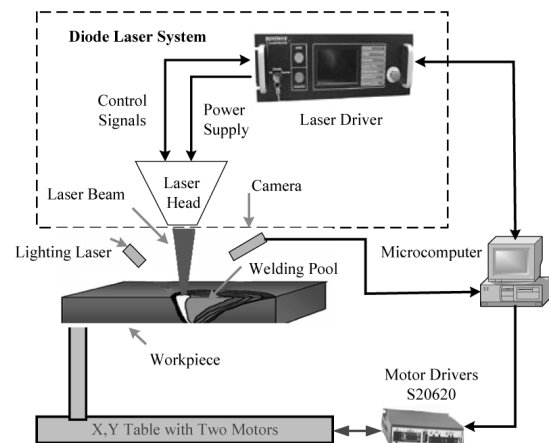
Experimental data contains more useful and direct information for control system design. It is well known that neural networks can memorise input–output correlation information that can be retrieved later. This implies that information obtained from experimental data

can be used in the form of trained neural networks in the welding process control. In this work, a Cerebellar Model Articulation Controller (CMAC) neural network-based two-input–two-output control system is designed to control the weld pool geometry using the real-time estimate of topside pool width and the estimated backside bead width as the feedback of the welding process.

2 Process

Figure 1 shows the HPDDL welding and control system. The laser head is powered with the drive, which is modulated and adjusted by the laser driver. The laser beam heats the workpiece on a moving table and forms a molten weld pool on the workpiece. The weld is formed after the molten pool is solidified.

Figure 1 HPDDL welding and control system



The major adjustable welding parameters include the welding speed, laser drive current and laser beam angle to travel direction on horizontal plane where workpiece lies. For ordinary use of the laser, the current is set at a fixed value through a panel screen of the laser driver despite the variations in other parameters. For use in real-time modulating laser power, a control interface on the rear of the laser driver can be used to adjust the current by changing the direct voltage applied on the interface. The welding speed can also be changed by means of a precision drive connected to the servo motor, which powers the movable table. In this work, the control signals of laser drive current and welding speed comes from the microcomputer. The computer also receives the image of the weld pool, illuminated by 223-nm pulse laser, from an image acquisition card connected to a high-shutter-speed camera controller. During welding, real-time image processing yields weld pool geometries to monitor/control the welding quality.

In this study, the laser beam is set at a fixed angle, welding speed and laser drive current are selected as control variables. The controlled process can therefore be defined as a HPDDL welding process in which the laser driver current and travel speed are modulated online to obtain the desired backside and topside widths of weld pool. The objective of this research is to design an online controller with good robust performance.

3 Experimental data analysis and process modelling

3.1 Calculation method of weld pool area

As the length of laser beam that focuses on workpiece is much greater than the desired topside weld pool width, the laser beam needs to have an angle of θ rather than 90° with respect to the welding direction on the plane where the workpiece surface lies. From experiments under different drive currents and welding speeds, one can obtain geometry of weld pool as shown in Figures 2 and 3.

Figure 2 Weld pools with different laser drive current. Speed: 3.86 mm/s; laser beam angle: 38° , 1 mm stainless steel; (a) 33.1; (b) 35.3; (c) 37.7 and (d) 39.5 A

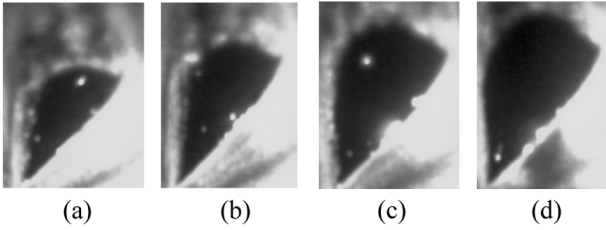
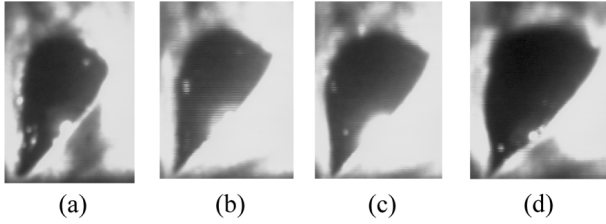


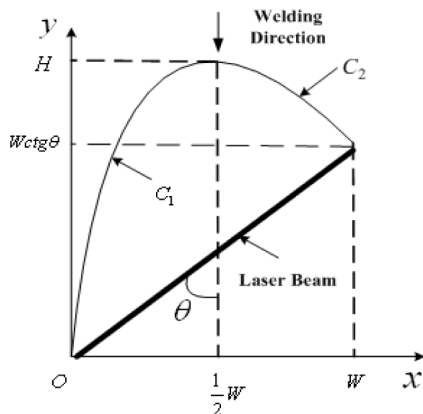
Figure 3 Weld pools at different welding speeds. Current: 35 A; laser beam angle: 38° , 1 mm stainless steel; (a) 4.43; (b) 3.87; (c) 3.3 and (d) 2.74 mm/s



Taking a careful look at the laser weld pools, it can be found that these pools have a similar boundary like a half peach, as shown in Figure 4. The boundary can be approximately expressed by two curves and one line, denoted as C_1 , C_2 and L_1 :

$$\begin{aligned} C_1 : y &= a_1x^2 + b_1x, & 0 \leq x \leq W/2 \\ C_2 : y &= a_2x^2 + b_2x + c_2, & W/2 \leq x \leq W \\ L_1 : y &= xctg\theta \end{aligned} \quad (1)$$

Figure 4 Description of typical weld pool boundary



From Figure 4, points $(0, 0)$ and $(W/2, H)$ lie on C_1 ; $(W/2, H)$ and $(W, Wctg\theta)$ on C_2 , and the maximal value on the two curves is approximately obtained at point $(W/2, H)$. The parameters in C_2 and C_1 can thus be determined:

$$\begin{aligned} a_1 &= -\frac{4H}{W^2}, \quad b_1 = \frac{4H}{W}; \quad a_2 = -\frac{4(H - Wctg\theta)}{W^2} \\ b_2 &= \frac{4(H - Wctg\theta)}{W}, \quad c_2 = Wctg\theta \end{aligned} \quad (2)$$

The area of the weld pool bounded by C_1 , C_2 and L_1 is

$$\begin{aligned} S &= \int_0^{W/2} (a_1x^2 + b_1x - xctg\theta) dx \\ &+ \int_{W/2}^W (a_2x^2 + b_2x + c_2 - xctg\theta) dx \end{aligned} \quad (3)$$

Substituting the parameters in C_1 , C_2 and L_1 into Equation (3) yields

$$S = \frac{1}{3}W(2H - Wctg\theta) = h(H, W, \theta) \quad (4)$$

The equation above can be used to calculate the weld pool area easily and quickly to reduce the image processing time.

3.2 Correlation between weld pool geometry and welding parameters

Extensive experiments have been performed under different laser driver currents (I) and welding speed (V) to study possible relationship between the backside bead width W_b and the topside weld pool geometry. Figure 5 plots experimental data on how the weld pool geometrical parameters change with increasing current at a few typical given speeds.

As seen in Figure 5, $R_{sw} = S/W_b$ changes very little as the current increases, although the topside weld pool width, backside bead width and weld pool area change rapidly. However, when the welding speed increases from $V = 2.74$ mm/s (Figure 5(a)) to $V = 4.31$ mm/s (Figure 5(d)), R_{sw} increased significantly. Define \bar{R}_{sw} as the average R_{sw} for a given speed, \bar{R}_{sw} can be considered a welding speed-dependent parameter, $\bar{R}_{sw}(V)$. \bar{R}_{sw} 's related to welding speeds are given in Table 1, and the correlation between them can be seen in Figure 6 that \bar{R}_{sw} has a nearly perfect linear relationship with V when welding conditions satisfy $30A \leq I \leq 40A$, 2.74 mm/s $\leq V \leq 4.98$ mm/s, and workpiece is fully penetrated and not burnt-through. This linear relationship is

$$\bar{R}_{sw} = a_3V + b_3 \quad (5)$$

where $a_3 = 2.81$ sec, $b_3 = 2.35$ mm. Substituting $\bar{R}_{sw} \approx R_{sw} = S/W_b$ into Equation (5) gives

$$W_b = \frac{S}{a_3V + b_3} = \frac{h(H, W, \theta)}{a_3V + b_3} = f(H, W, V, \theta) \quad (6)$$

Hence, the backside bead width W_b can be accurately estimated from the topside weld pool area of S and the weld speed of V .

Figure 5 Experimental data: (a) $V = 2.74$ mm/s, (b) $V = 3.41$ mm/s, (c) $V = 3.86$ mm/s and (d) $V = 4.31$ mm/s

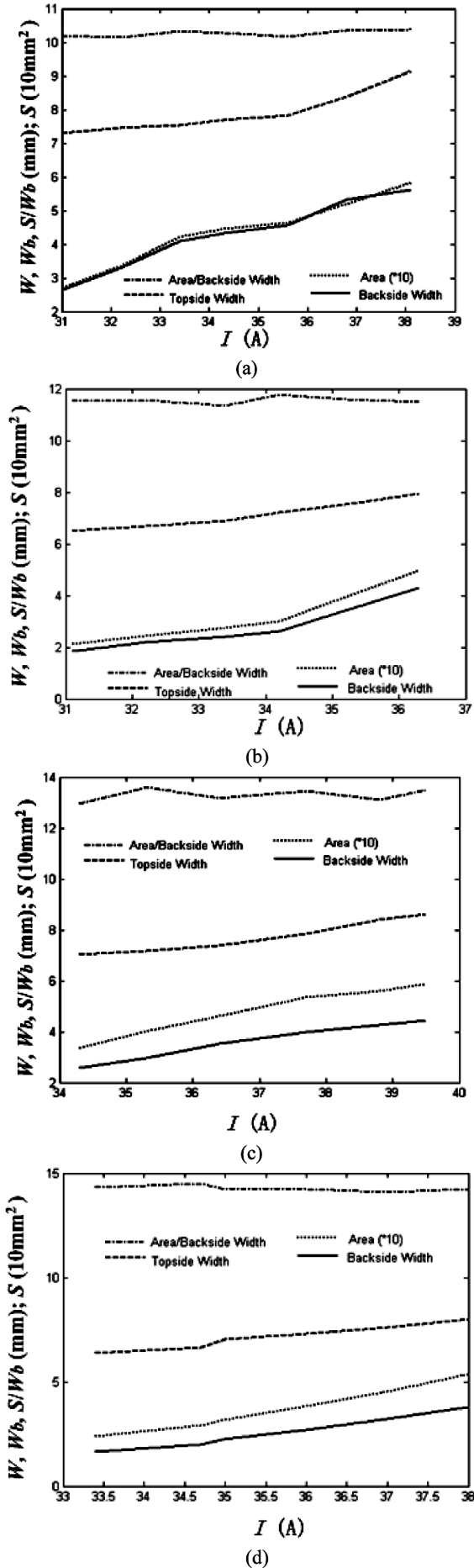
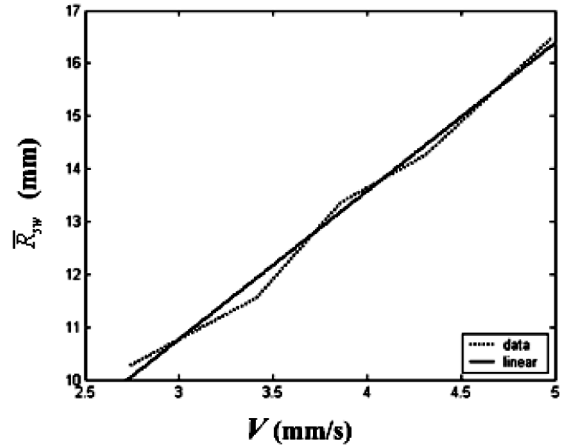


Table 1 \bar{R}_{sw} at typical values of speed

V (mm/s)	2.74	3.41	3.86	4.31	4.98
\bar{R}_{sw} (mm)	10.27	11.55	13.37	14.27	16.48

Figure 6 Correlation between V and \bar{R}_{sw}



3.3 CMAC neural network-based modelling

3.3.1 Existence condition of inverse process model

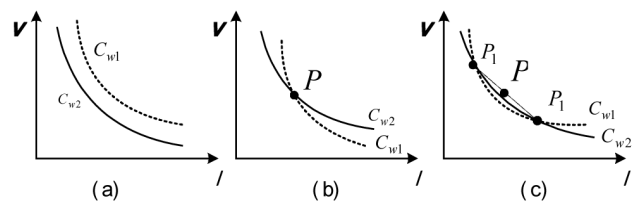
Experimental data show that both W and W_b increase with the increasing current I when the speed is constant, and decreases with the increasing speed V when the current remains unchanged. This concurs with the physical process.

Suppose the existence of steady-state input–output correlation is depicted by

$$\begin{cases} W = f_1(I, V, \theta_0) \\ W_b = f_2(I, V, \theta_0) \end{cases} \quad (7)$$

where θ_0 is a constant laser beam angle to the welding direction. If V is a constant V_0 , then $W = f_1(I, V_0, \theta_0)$ and $W_b = f_2(I, V_0, \theta_0)$ monotonously increase with I . Similarly, $f_1(I_0, V, \theta_0)$ and $f_2(I_0, V, \theta_0)$ for a fixed I_0 monotonously decrease with V . Further, for physically reasonable values of $W = W^*$ and $W_b = W_b^*$, the $V \sim I$ curves defined by $W^* = f_1(I, V, \theta_0)$ and $W_b^* = f_2(I, V, \theta_0)$ are monotonous and denoted as C_{w1} and C_{w2} , respectively. Figure 7 shows their possible spatially intersectional relationship.

Figure 7 Three possible intersectional relationship between C_{w1} and C_{w2}



In Figure 6(a), there is no intersection between C_{w1} and C_{w2} . This implies that the given W_b^* and W^* cannot be physically realisable at the same time. In Figure 7(b), there

is only one physically realisable solution at the point P . In Figure 7(c), two intersections P_1 and P_2 exist and there are two pairs of current and speed, which can produce the desired values (W_b^* , W). Therefore, adjusting the control variables is to obtain the desired values of W_b and W . The ideal situation would be that the values of control variables can be known at once when the desired W_b and W are given or changed. Hence, to design the controller could become to get a solution to equation

$$\begin{cases} W^* = f_1(I, V, \theta_0) \\ W_b^* = f_2(I, V, \theta_0) \end{cases} \quad (8)$$

and the approximate values can be found by modelling the inverse laser welding process.

CMAC neural network combined with general basis function has many advantages such as fast learning and perfect generalisation ability (Chiang and Lin, 1996). For easy use of the CMAC and choosing parameters in learning algorithm, the CMAC structure and learning algorithm need to be modified.

3.3.2 CMAC structure and learning algorithm

Suppose system input vector is

$$x \in U = A_1 \times A_2 \times \dots \times A_n$$

where $A_i = [\text{Min}_i, \text{Max}_i]$ is i th dimensional input interval to be considered. If each input interval is quantised into M_i levels, there are L intersectional points $p_j = [p_{j,1}, p_{j,2}, \dots, p_{j,i}, \dots, p_{j,n}]$, $p_{j,i} \in A_i$, to be named as crossed nodes. The hyper-ball C_j , whose centre is p_j , is defined as

$$C_j = \left\{ x \mid \prod_{i=1}^n |x_i - p_{j,i}| \leq R_{a,i} \right\}, \quad j = 1, 2, \dots, n \quad (9)$$

The quantisation method is shown as in Figure 8. Suppose there are L Gauss basis functions $b_j(x)$ to be defined for $x \in C_j$, given as

$$b_j(x) = \begin{cases} \exp\left[-\sum_{i=1}^n (x_i - p_{j,i})^2 / \sigma_i^2\right], & x \in C_j \\ 0, & x \notin C_j \end{cases} \quad (10)$$

If $\forall x_k \in S_s$, S_s is a learning sample set, then there will be N_e crossed nodes to be included in the hyper-balls $C_{k,m}$, $m = p_k, q_k, \dots, r_k$ and p_k, q_k, \dots, r_k are the sequence numbers to denote the positions of these included crossed nodes. The index vector S_k , whose factors are consisted of zero and one to denote whether the corresponding sequence hyper-balls including x or not, written as $S_k = [0, 0, \dots, 1, 0, \dots, 0, 1, 0, \dots, 1, 0, \dots, 0]^T$. Therefore, there are N_e 1s in S_k . Denoting $B(x_k) = \text{diag}[b_1(x_k), b_2(x_k), \dots, b_L(x_k)]$ and related parameter vector $q = [q_1, q_2, \dots, q_L]^T$, the CMAC output is

$$\hat{y}_{k+1} = S_k^T B(x_k) q = \sum_{i=1}^L S_{k,i} b_i(x_k) q_i = \sum_{i \in I_k} b_i(x_k) q_i \quad (11)$$

where $I_k = \{p_k, q_k, \dots, r_k\}$. The mapping correlation between the input and output using the equation above is shown as in Figure 9.

Figure 8 Three-dimensional input quantisation

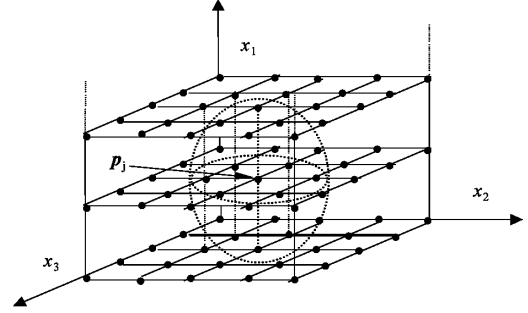
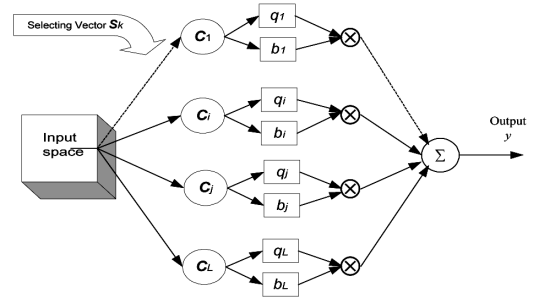


Figure 9 Hyper-ball CMAC structure



The model identification is to seek q , the only unknown parameter in Equation (11). If there is a sample set $S_a = \{(y_{i+1}, x_i)\}$, one can use the adaptive learning algorithm (Duan and Shao, 1999)

$$\Delta q_{k-1} = \frac{\alpha e_{k-1} B(x_{k-1}) S_{k-1}}{\beta + S_{k-1}^T B(x_{k-1}) B^T(x_{k-1}) S_{k-1}} \quad (12)$$

where α and β are given constants for a specific non-linear dynamic system and $e_{k-1} = y_{k-1} - \hat{y}_{k-1}$. The learning process is shown in Figure 10.

One time of picking up all sample data in sequence and respectively learning the data to adjust the weight vector is called one time of iteration, and picking up called a sample a pick-up. Denote the k th sample estimated error at i th iteration as

$$e_k^{(i)} = y_k - \hat{y}_k^{(i)} \quad (13)$$

where y_k and $\hat{y}_k^{(i)}$ are desired and estimated outputs with input x_k , respectively. Let $q_k^{(i)}$ be the weight parameter vector before the k th sample is learned to adjust it at i th iteration, $\hat{y}_k^{(i)}$ can be obtained as using (11):

$$\hat{y}_k^{(i)} = S_k^T B(x_k) q_k^{(i)} \quad (14)$$

Summarising adjusting process with (12) and (13) yields the adjusting algorithm of weight vector given as

$$\begin{cases} q_k^{(i)} = q_{k-1}^{(i)} + \Delta q_{k-1}^{(i)}, & k = 2, 3, \dots, N_s \\ q_1^{(i+1)} = q_{N_s}^{(i)} + \Delta q_{N_s}^{(i)} \\ \Delta q_{k-1}^{(i)} = \frac{\alpha}{\beta + f_{k-1}} e_{k-1}^{(i)} B(x_{k-1}) S_{k-1} \end{cases} \quad (15)$$

where

$$f_{k-1} = S_{k-1}^T B(x_{k-1}) B^T(x_{k-1}) S_{k-1} = \sum_{l \in I_{k-1}} b_l^2(x_{k-1})$$

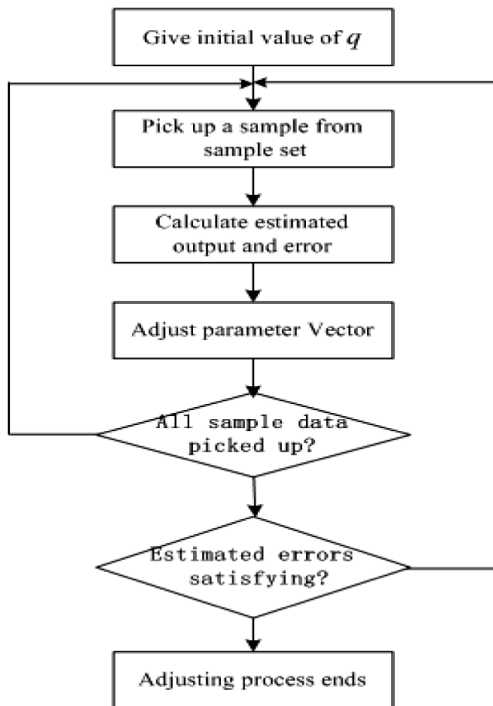
Specially, $q_1^{(0)} = q_0$ is the initial value.

Denote $q_k^{(i+1)} = q_k^{(i)} + Dq_k^{(i)}$, one can have the following theorem that means the learning algorithm above is convergent if iteration learning time approaches infinite.

Theorem: If $0 < \alpha < 2$, $\beta > 0$ $\lim_{j \rightarrow +\infty} Dq_k^{(j)} = 0$

The theorem above can be proved in the similar way to the one used in Duan and Shao (1999).

Figure 10 Parameter adjusting process



3.3.3 CMAC-based process model

Using the CMAC presented above, one can model the process through sample data learning.

Model 1: Topside weld pool width. The CMAC's inputs are the current and speed, the output is the topside weld pool width. Its input subset $U = [28, 42] \times [2.75, 4.98]$, and the learning sample data has format [topside width (current, speed)].

Model 2: Backside bead width. The CMAC's inputs and input subset are the same as *Model 1*. Its output is the backside bead width and the learning sample data format is [backside width (current, speed)].

Model 3: Laser driver current. CMAC's inputs are topside and the backside weld bead widths. Its output is the laser driver current. The input subset $U = [5, 9] \times [2, 6]$, the learning sample data format is [current (topside width, backside width)].

Model 4: Welding speed. The CMAC's inputs and input subset are the same as *Model 3*. Its output is the welding speed. The learning sample data has format [speed (topside width, backside width)].

In each CMAC model above, every dimensional input is equally quantised into seven levels including its minimum and maximum values, and the value of σ in basis function for each dimension is 0.77 times length of one level. $\alpha = 1.2$, $\beta = 0.05$.

After having learnt respective sample data 20 times, *Models 1–4* memorised corresponding information from experimental data. In addition, these CMACs have good performances on estimating the output of an input among adjacent sample inputs in acceptable accuracy because of their great generalisation abilities. It is evident that the welding process with two outputs, expressed by *Model 1* as shown in Figure 11(a) and *Model 2* as shown in Figure 11(b), is a non-linear system, also it is difficult to depict the process using a physical parameter model. The inverse models, *Models 3 and 4* to be used to design controller, is shown in Figure 12(a) and (b), respectively.

It should be noted that not all input subsets in Figures 11 and 12 are effective and physically reasonable, because too low speed and too high current will make workpiece burnt-through, or too low current and too high speed will produce partial penetration. Although there is no knowledge of sample data in these input areas, the CMAC still generates an unreasonable output with respect to an output on these impossible areas because of CMAC generalisation. Take Figure 12(b) for example, the speed cannot be negative. By doing experiment, one can easily find the reasonable input area.

Another fact that needs to be analysed is that if the situation as shown in Figure 7(c) exists, *Models 3 or 4* can estimate average values given by P theoretically close to the middle between P_1 and P_2 because of data fusion during CMAC learning experimental data set that includes samples obtained in this situation.

Figure 11 CMAC-based models: (a) topside weld pool width and (b) backside weld bead width

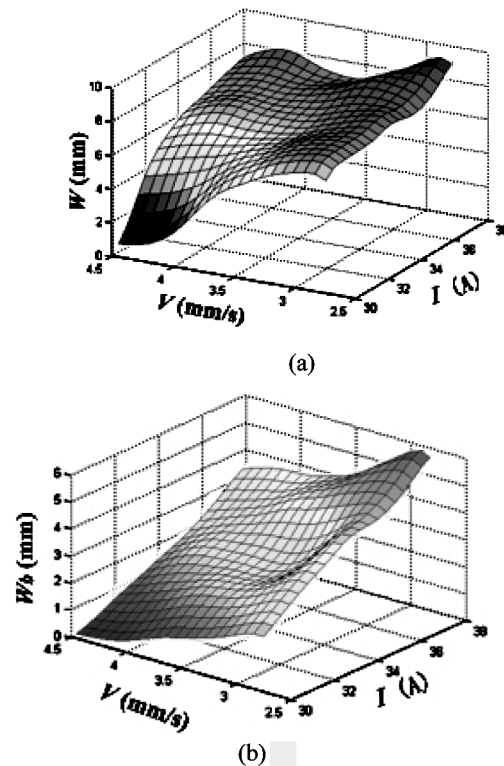
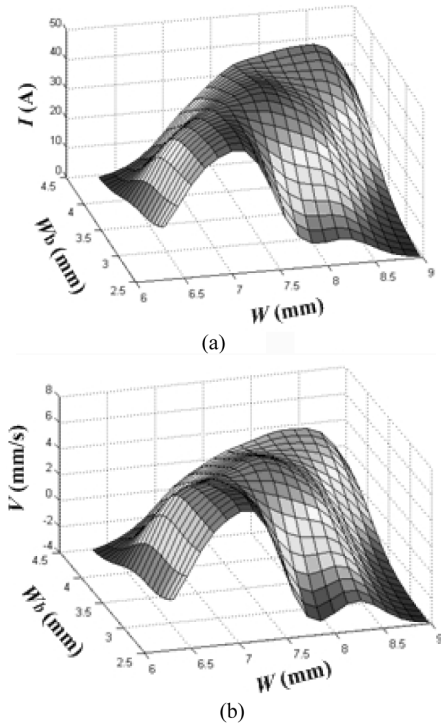


Figure 12 CMAC-based inverse models: (a) laser driver current and (b) welding speed



4 Closed-loop control strategy and simulation experimental results

The purpose of the control strategy is to design a control algorithm to search for the proper values of laser driver current and welding speed that can work on the process to produce a desired topside and backside weld pool width using as much information from the experimental data as possible. Therefore, *Models 3* and *4* are used as control variable estimators to estimate the current and speed according to the set points of outputs, as shown in Figure 13. Because there is possible inaccuracy of models or disturbance in control system, these estimators alone may not achieve the outputs at desired levels. Real-time feedbacks have to be considered. Some characteristics of the laser process can help use Proportional and Integral (PI) controller to compensate the possible inaccuracy and disturbance.

The topside pool width changes earlier, faster and more directly than the backside bead width when the current varies, whereas the topside pool width is more sensitive to the change in the current than topside pool width, as

shown in Figure 11. In addition, either increasing the current or decreasing the welding speed widens both topside pool and backside bead widths simultaneously, but to different levels. On the basis of these characteristics of the process, I is used to mainly adjust W , and V to W_b . The frame of CMAC model-based intelligent control system that has been designed and implemented is shown in Figure 13, where $f(V_k, H_{k+1}, W_{k+1})$ can be considered as a soft sensor to indirectly measure the backside bead width. The control system applies *Models 3* and *4* as the predictive estimators for initial speed and current according to the set point, and uses two feedback closed loops including the topside pool width loop and the backside bead width loop.

At instant k , the output of PI controller one, $u_{1,k}$, can make a compensation for the error between the required speed and estimated value $u_{2,k}$ in order that backside bead width is its set point $W_{b0,k}$. This error may occur due to inaccuracy of the estimated value $u_{2,k}$ or because of disturbances. Similarly, another PI controller's output $u_{4,k}$ overcomes the influence of inaccuracy of the estimated value $u_{5,k}$ or from disturbances in order that the topside weld pool width is its set point $W_{0,k}$.

For testing the closed-loop control system developed, simulation experiments have been performed under three different welding conditions.

4.1 No disturbance

During the first 35 sec, the nominal value of speed (Figure 14(a)) is exactly the same as the actual ones (Figure 14(b)), and the nominal value of current (Figure 14(c)) equals the actual value of current (Figure 14(d)). The welding process' outputs (weld pool topside width (Figure 14(e)) and weld pool backside bead width (Figure 14(f))) show that the designed controller can maintain the outputs at the desired levels.

4.2 Current disturbance

At $t = 35$ sec, an artificial error between the nominal and actual values of the current is introduced. The actual current 1 A less than nominal value leads to the decreases in topside and backside widths, shown as in Figure 14(e) and (f). As seen in Figure 14(a) and (c), the nominal current and speed immediately increases and decreases, respectively, to eliminate the error's influence. In a short time, the actual values of current and speed reached the values before the occurrence of disturbance as shown in

Figure 13 Frame of CMAC model-based intelligent control

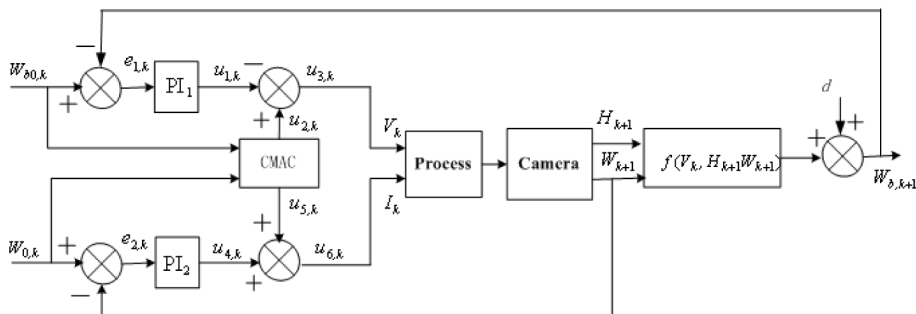
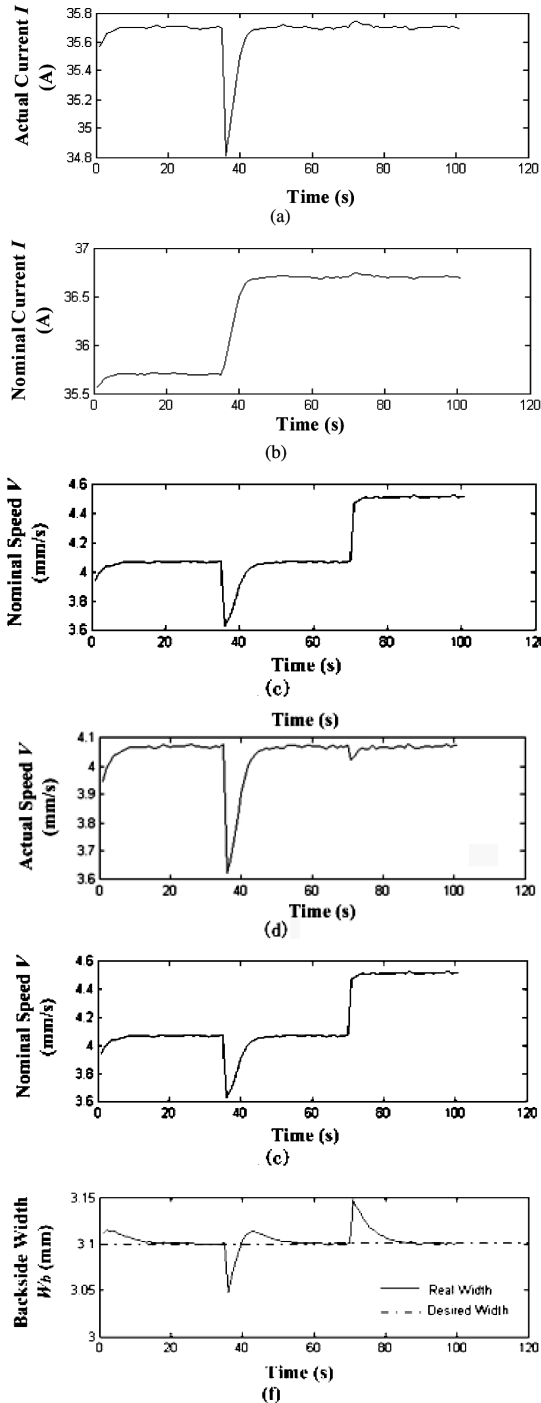


Figure 14(b) and (d), so that the outputs returned to the initial states before the error occurs. It is noted that this artificial disturbance indicates the process model is changed, because it alters the correlation of outputs to the nominal values of welding parameters. Therefore, a model perturbation coming from current input is emulated.

Figure 14 Real-time closed-loop control result: (a) nominal current, (b) actual current, (c) nominal speed, (d) actual speed, (e) topside weld pool width and (f) backside bead width



4.3 Speed disturbance

At $t = 70$ sec, an artificial error between the nominal and actual values of the speed occurs. The actual speed 0.5 mm/s less than nominal value causes the increases in topside and backside widths. As shown in Figure 14(c), the

nominal speed increases at once. After a while, the actual values of current and speed reaches the desired values again, so that the outputs are their own set points. This part of the experiment emulates the influence of inaccuracy of model resulted from speed input channel.

5 Conclusions

The fundamental issue is that the physical parameter model of the controlled process with two inputs including the laser driver current and welding speed as well as two outputs, topside and backside bead widths, is unknown. The Gauss function-based CMAC neural network can act as the inverse model of the controlled process after viewing the experimental data obtained under various welding conditions. A CMAC model-based on double-closed-loop control system can control the non-linear laser welding process. The control simulation experiments with disturbances demonstrate that the welding geometry determining the welding quality can be controlled with sufficient accuracy using the developed control system.

The method of the controller design provides a simple and easy solution to precision control of HPDDL welding process. Although the laser beam angle remains unchanged in this work, it may also be thought as one variable to increase the control flexibility.

Acknowledgement

This work is financially supported by the Natural Science Foundation of Shandong Province, China (Grant No. Q2002G01) and the National Science Foundation under DMI-0527889.

References

- Bagger, C. and Olsen, F.O. (2003) 'Laser welding closed-loop power control', *Journal of Laser Applications*, Vol. 15, No. 1, pp.19–24.
- Bardin, F., Cobo, A., Lopez-Higuera, J.M., Collin, O., Aubry, P., Dubois, T., Hogstrom, M., Nysten, P., Jonsson, P., Jones, J.D.C. and Hand, D.P. (2005) 'Closed-loop power and focus control of laser welding for full-penetration monitoring', *Applied Optics*, Vol. 44, No. 1, pp.13–21.
- Chiang, C-T. and Lin, H-S. (1996) 'CMAC with general basis functions', *Neural Networks*, Vol. 9, No. 7, pp.1199–1211.
- Duan, P. and Shao, H. (1999) 'Improved algorithm of CMAC with general basis function and its convergence analysis', *Zidonghua Xuebao/Acta Automatica Sinica*, Vol. 25, No. 2, pp.258–263 (in Chinese).
- Kawahito, Y. and Katayama, S. (2004) 'In-process monitoring and feedback control during laser microspot lap welding of copper sheets', *Journal of Laser Applications*, Vol. 16, No. 2, pp.121–127.
- Meijer, J., Postma, S., Aarts, R.G.K.M. and Jonker, J.B. (2002) 'Penetration control in laser welding of sheet metal', *Journal of Laser Applications*, Vol. 14, No. 4, pp.210–214.
- Zhang, Y.M. and Kovacevic, R. (1998) 'Neurofuzzy model-based predictive control of weld fusion zone geometry', *IEEE Transaction on Fuzzy Systems*, Vol. 6, No. 3, pp.389–401.